

Realistic observing scenarios for the next decade of early warning detection of binary neutron stars

RYAN MAGEE¹ AND SSOHRAB BORHANIAN²

¹LIGO, California Institute of Technology, Pasadena, CA 91125, USA

²Theoretisch-Physikalisches Institut, Friedrich-Schiller-Universität Jena, D-07743 Jena, Germany

ABSTRACT

We describe realistic observing scenarios for early warning detection of binary neutron star mergers with the current generation of ground-based gravitational-wave detectors as these approach design sensitivity. Using Fisher analysis, we estimate that Advanced LIGO and Advanced Virgo will detect one signal before merger in their fourth observing run provided they maintain a 70% duty cycle. 60% of all observations and 8% of those detectable 20 seconds before merger will be localized to $\lesssim 100$ deg². If KAGRA is able to achieve a 25 Mpc horizon, these prospects increase to $\lesssim 2$ early detections with 70% of all BNS localized to $\lesssim 100$ deg² by merger. As the AHKLV network approaches design sensitivity over the next ~ 10 years, we expect up to 1 (14) detections made 100 (10) seconds before merger. Although adding detectors to the HLV network impacts the detection rate at $\lesssim 50\%$ level, it improves localization prospects and increases the completeness of compact binary surveys. Given uncertainties in sensitivities, participating detectors, and duty cycles, we consider 103 future detector configurations so electromagnetic observers can tailor preparations towards their preferred models.

1. INTRODUCTION

Advanced LIGO (Aasi et al. 2015), Advanced Virgo (Acernese et al. 2015), and KAGRA (Akutsu et al. 2019) have enjoyed remarkable success since the first detection of gravitational waves (GWs) from a binary black hole merger in 2015 (Abbott et al. 2016). Since then, analyses by the LIGO-Virgo-KAGRA collaboration (LVK) have uncovered a growing population of binary black holes, binary neutron stars (BNSs), and neutron star - black hole binaries (NSBHs) (Abbott et al. 2019, 2021a,b,c). Analyses of public data (Trovato 2020) have confirmed many of these detections and hinted at other promising candidates lurking deeper in the noise (Nitz et al. 2019; Magee et al. 2019; Zackay et al. 2019; Venumadhav et al. 2020; Nitz et al. 2020b, 2021; Olsen et al. 2022).

GW observations coincident with other astrophysical signals such as electromagnetic radiation or particles are a highly sought-after subclass of so-called *multi-messenger* detections. Even before the first detection of GWs, various studies investigated what to expect from electromagnetic follow-up efforts during the Advanced LIGO and Advanced Virgo era (Cannon et al. 2012; Singer et al. 2014). The first multi-messenger detection with GWs, GW170817 (Abbott et al. 2017a,b), was serendipitous in nature, and led to an explosion in works focused on facilitating additional discoveries.

In particular, there has been an increasing focus on *early warning* (or pre-merger) detection and localiza-

tion of BNSs and NSBHs (Sachdev et al. 2020; Nitz et al. 2020a; Singh et al. 2021; Yu et al. 2021; Tsutsui et al. 2021; Kovalam et al. 2021). Several of these works, in particular (Sachdev et al. 2020; Nitz et al. 2020a; Singh et al. 2021; Kovalam et al. 2021), focus on BNS detection for the current generation of ground-based detectors, though many optimistically assume a 100% duty cycle and sensitivities that may prove difficult to reach (Akutsu et al. 2019; Washimi et al. 2021). More recently, there has also been a focus on the infrastructure necessary to realize early warning alerts with an emphasis on latencies expected in the LVK's fourth observing run (O4) (Magee et al. 2021).

In this study, we investigate projected observing scenarios of current generation ground-based detectors for early warning detection using well-established Fisher analysis techniques (Finn & Chernoff 1993; Finn 1992; Cutler & Flanagan 1994; Poisson & Will 1995; Balasubramanian et al. 1996). We extend previous studies of BNSs in three major ways. First, we estimate the localization for 103 combinations of detectors and detector sensitivities for Advanced LIGO, Advanced Virgo, and KAGRA in O4 as well as at their projected *design* sensitivity (referred to as O5). Second, we provide the probability density distributions of the 90%-credible sky area as a function of early warning time to enable the consideration of arbitrary network combinations, duty factors, and early warning detection times. We compare our results to similar work previously carried out (Sachdev et al. 2020; Nitz et al. 2020a; Abbott et al. 2020b). Fi-

nally, we include the impact that the KAGRA detector would have at three projected and one realized sensitivity in light of recent construction difficulties (Akutsu et al. 2019; Washimi et al. 2021).

2. METHODS

Bayesian approaches such as full parameter estimation (Veitch et al. 2015; Ashton et al. 2019) and the `bayestar` code (Singer & Price 2016) are presently used to provide the most accurate localizations possible for compact binary mergers. Although full parameter estimation is accurate, it takes $\mathcal{O}(\text{hours-days})$. `bayestar` does not sample over the masses or spins of the binary and is able to provide comparable localizations in $\mathcal{O}(1 \text{ second})$ when run in parallel (or $\mathcal{O}(1 \text{ minute})$ on a single thread). Singer et al. (2014) showed that the two methods largely agree with each other.

For large trade studies, Fisher analysis methods are often favored since they only depend on the characteristics of the gravitational waveform model and detectors under investigation. They provide a simple and fast way of estimating the information a signal contains on the waveform model’s parameter domain. Here, we use the Fisher analysis-based software package `gwbench` (Borhanian 2020) to benchmark the measurement capabilities of 103 detector network configurations detailed in the next section. Since this study is focused on BNS signals which do not merge in the most sensitive bands of current generation detectors, we consistently employ a simple inspiral waveform model, TaylorF2 (Sathyaprakash & Dhurandhar 1991; Blanchet et al. 1995, 2005; Buonanno et al. 2009) to estimate the expected measurement uncertainties for the following parameters: $\mathcal{M}, \eta, D_L, t_c, \phi_c, \iota, \psi, \alpha, \delta$. These denote the chirp mass, symmetric mass ratio, luminosity distance, coalescence time, coalescence phase, inclination, polarization angle, right ascension, and declination, respectively. Finally, we can estimate the uncertainty in sky localization via the 90%-credible sky area following Cutler (1998) and Barack & Cutler (2004) as

$$\Delta\Omega_{90} = 2\pi \ln(10) |\cos \delta| \sqrt{\text{Var}(\alpha)\text{Var}(\delta) - \text{Cov}^2(\alpha, \delta)} \quad (1)$$

where $\text{Var}(\alpha)$ and $\text{Var}(\delta)$ are the variances of the right ascension and declination, respectively, and $\text{Cov}(\alpha, \delta)$ is the covariance between the right ascension and declination. There are, however, several limitations to Fisher analysis approaches (Vallisneri 2008; Rodriguez et al. 2013). Most well-known is that they are only valid in the high signal-to-noise ratio (SNR) limit ($\gtrsim 10$ per detector) (Vallisneri 2008). Further, special considerations are necessary while interpreting sky localizations: Fisher

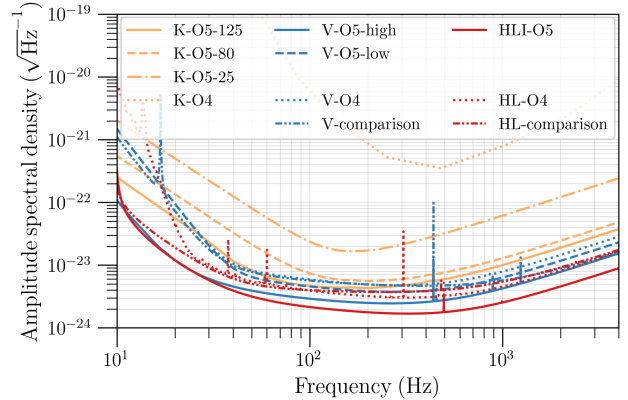


Figure 1. The amplitude spectral densities (ASD) assumed for this trade study. With the exception of the O4 KAGRA ASD that was obtained through digitization of Figure 1 from Washimi et al. (2021), all other ASDs are obtained from the observing scenarios data release. ASDs are labeled as they appear in the data release and/or in the publicly provided estimates in LIGO-T2000012.

analyses estimate the overall uncertainty and therefore cannot estimate proximity of regions of probability in the sky. Additionally, they can exhibit mirror degeneracies (Fairhurst 2009) and scale differently with the SNR than coherent Bayesian approaches (Berry et al. 2015). As Cannon et al. (2012) noted, Fisher analysis estimates tend to be optimistic. We quantify this bias of our approach in comparison to `bayestar` in Section 4.1.

We do not impose any single detector SNR thresholds; note that this means low SNRs in one detector can contribute to the network SNR threshold used as a detection criterion. In practice, we expect the bias introduced by this effect to be small. Unless otherwise noted, we assume a network SNR detection threshold of 15. In all cases, we conservatively assume that no localizations can be provided when only one detector is operating.

3. POPULATION AND NETWORKS

Binary neutron star population—Although two probable NSBH systems were recently observed by Advanced LIGO and Advanced Virgo (Abbott et al. 2021d), we restrict the analysis here to BNS populations due to uncertainties in the NSBH population and poor early warning and localization prospects for NSBHs. We consider the same astrophysically motivated source population of BNSs as in (Sachdev et al. 2020). The source-frame component masses are drawn from a Gaussian distribution with mean mass $1.33M_\odot$ and standard deviation $0.09M_\odot$. The source-frame masses are further limited such that $1.0M_\odot < m_2 < m_1 < 2.0M_\odot$. This population is modeled after galactic observations of BNS (Özel & Freire 2016). We note that the masses inferred from

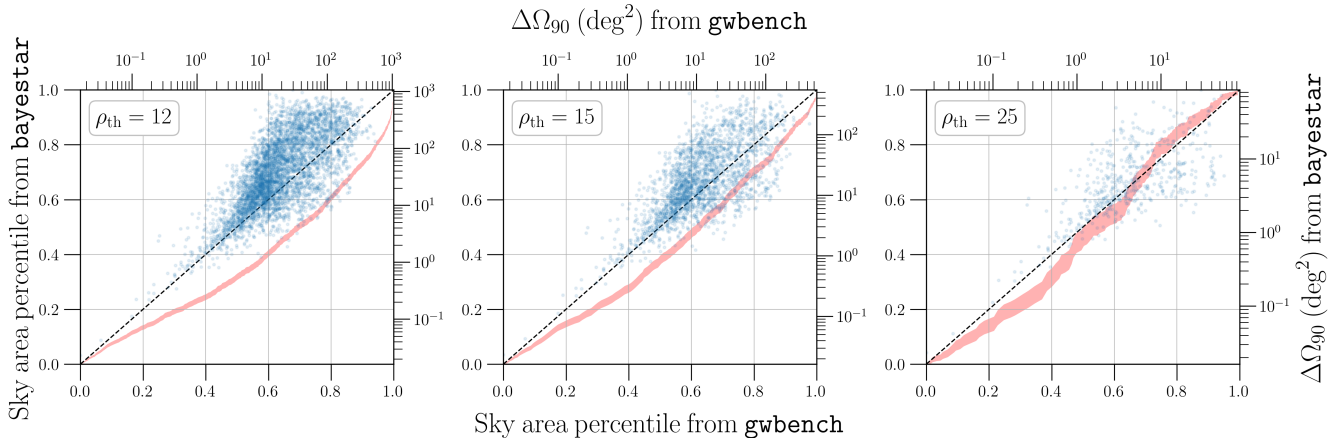


Figure 2. A comparison of the 90% confidence interval computed by `bayestar` vs. the Fisher matrix formalism used here (`gwbench`) for events with network SNR thresholds ρ_{th} of 12, 15, and 25. Each point represents a localization measurement obtained by both `bayestar` and `gwbench`. Note that the high SNR (small localization) events largely agree, but that this agreement becomes statistical in nature for larger areas. The bias between these two methods is more easily visible in the overlaid *pp*-plot comparing the 90%-credible sky area percentiles obtained by `gwbench` and `bayestar`. We include uncertainties on the percentiles measured due to the size of our population, which is dependent on the SNR threshold used. We find that `gwbench` systematically underestimates the size of the confidence interval at SNR 12.

GW190425 (Abbott et al. 2020a) are in tension with this population. This could be an indication that galactic measurements are not representative of the broader population of neutron stars. Results from the LVK’s recent population analysis seems to support this claim (Abbott et al. 2021e). We neglect these uncertainties here and naively apply the most recent BNS merger rate estimates (Abbott et al. 2021e) to our population, though we note that (1) our method can be quickly rerun to produce estimates for arbitrary populations, (2) that as pointed out in Nitz et al. (2020a), our results can be scaled to systems of arbitrary mass, and (3) that expected BNS localizations do not appear to significantly depend on the specifics of the population (Pankow et al. 2020).

Networks—We examine 103 GW detector networks for O4 and O5 that arise from 11 different projected sensitivity curves, summarized in Figure 1. For O4, we consider combinations of Hanford-KAGRA-Livingston-Virgo (HKLTV) networks that contain at least two of the HLV detectors, with HLV sensitivities as described in the latest observing scenario¹. Perhaps the biggest question for O4 is the level to which KAGRA will be able to participate (LVK 2021). In this work, we consider two possible KAGRA sensitivities for O4 with 1 Mpc and 25 Mpc BNS detection horizons. We regard this to be a more realistic update to the recent O4 early warning

detection and localization estimates provided in Magee et al. (2021) which assumed a horizon of 80 Mpc, especially in light of the recent LVK announcement suggesting KAGRA will start O4 with 1 Mpc horizon (LVK 2021). The KAGRA sensitivities were digitized from Figure 1 in Washimi et al. (2021).

For O5, we consider a 5-detector network, AHLV including LIGO-Aundha (Saleem et al. 2022), previously LIGO-India (Iyer et al. 2011). Following Abbott et al. (2020b), we assume that Aundha, Hanford, and Livingston are all able to achieve comparable sensitivities (e.g. the Advanced LIGO design sensitivity). We compute all network combinations where at least two of the AHLV detectors are operating. We consider two separate, publicly available sensitivities for Virgo, and three sensitivities for KAGRA, assuming that by O5 KAGRA will achieve either 25 Mpc, 80 Mpc, or 125 Mpc BNS detection horizons outlined in the observing scenarios review.

4. RESULTS

4.1. Comparison to known localizations

In order to quantify any biases introduced by the Fisher analysis, we compare our localization estimates from `gwbench` to those computed by `bayestar` for all simulated signals recovered by the full search presented in Sachdev et al. (2020). Figure 2 shows a comparison of the 90%-credible sky area computed via each method at three network SNRs ρ_{net} (right and top axes), together with a *pp*-plot comparing the percentiles associated with each localization estimator (left and bottom axes). In

¹ We use the publicly provided PSDs: LIGO-T2000012.

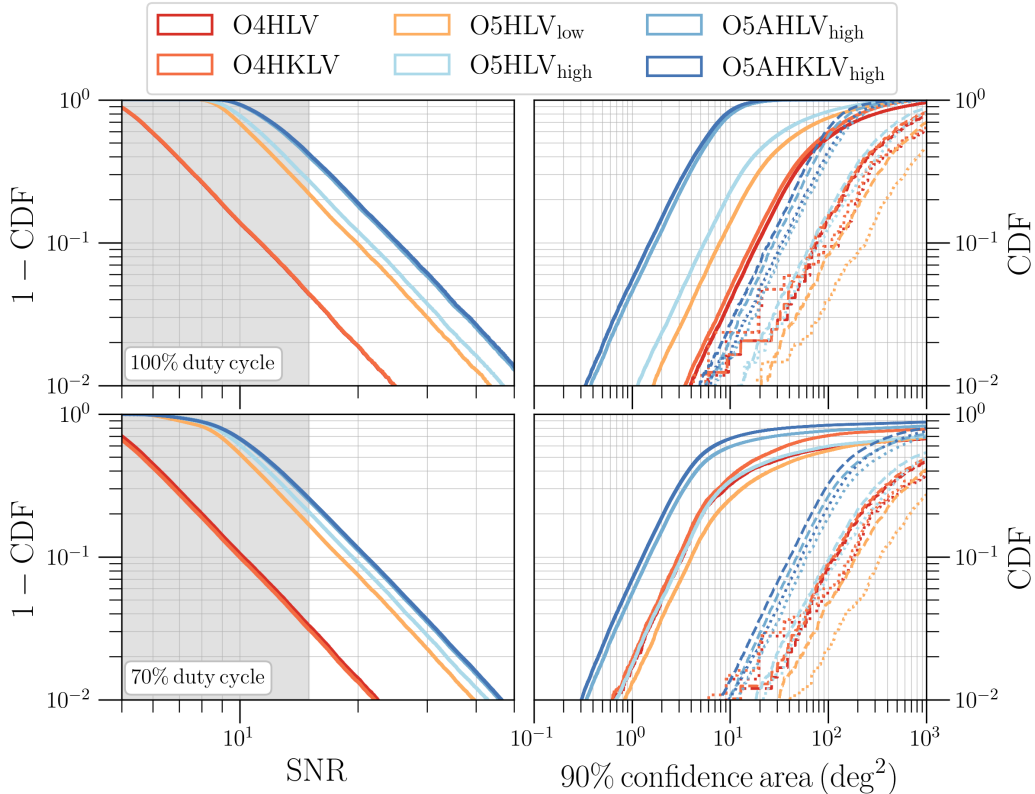


Figure 3. Cumulative SNR (left) and localization (right) distributions for six sample network configurations operating at 100% (top) and 70% (bottom) duty cycles. We include predictions for the early warning localization distributions obtained 0 s (solid), 20 s (dashed), and 40 s (dotted) before merger. The 70% duty cycle cumulative distributions assume single detector candidates are not localized (e.g. they are normalized to two or more detector networks).

general, we find that `gwbench` and `bayestar` agree to within a factor of a few depending on the SNR threshold used. At SNR 12, the 50th (90th) percentiles agree to within a factor of ~ 3 (~ 8). At SNRs 15 and 25, this improves to ~ 2 (~ 6) and < 2 (< 6), respectively.

Although localizations largely agree on the event-by-event level, we empirically find that at $\rho_{\text{net}} \lesssim 15$ there are significant biases between the expected localization distributions obtained when compared to `bayestar`. The *pp*-plots overlaid in Figure 2 show that, in general, the Fisher analysis systematically underestimates the size of the 90%-credible sky area. This effect lessens in severity as the SNR threshold is increased. For $\rho_{\text{net}} \geq 25$, the bias has mostly disappeared.

We assert that the statistical agreement between the two methods is trustworthy for systems with $\rho_{\text{net}} \geq 15$, and accurate to $\lesssim 1$ order of magnitude at lower SNRs. We therefore assume a detection threshold of $\rho_{\text{net}} \geq 15$ for the remainder of this work and assume the individual localizations produced are accurate to within a factor of a few.

4.2. O4

Figures 3 and 4 present the cumulative SNR and localization distributions and the expected yearly early warning detection rates, respectively, for six representative O4 and O5 networks: O4HLV, O4HKL, O5HLV_{low}, O5HLV_{high}, O5AHLV_{high}, and O5AHKL_{high}. We highlight two early warning times, 20 s and 40 s before merger, which are motivated by data analysis latencies (Magee et al. 2021) and approximate $\mathcal{O}(10\text{ s})$ slew times.

It was recently announced that KAGRA is expected to join O4 with a horizon of at least $\sim 1\text{ Mpc}$ (LVK 2021). As expected, we find that there is no impact on the network sensitivity and negligible impact on the localizations achieved when this HKLV network is compared to HLV. However, if KAGRA is able to reach 25 Mpc, we find an average $\sim 40\%$ reduction in the 90%-credible sky areas for events with $\text{SNR} \geq 15$, though the number of expected detections increases at less than the percent level, see Figure 3. Thus while a moderately sensitive KAGRA in O4 will not increase the number of detec-

tions, it will greatly improve the localization for existing detections.

As shown in Figure 4, early warning detections in O4 are likely to be exceedingly rare; we expect $\lesssim 1$ detection made to be made early enough to overcome analysis latencies (e.g. 20s early) per year. Of these observations, we expect 10 – 20% to have localizations $\lesssim 100\text{deg}^2$. The presence/absence of KAGRA has negligible impact on the localization or abundance of early warning detections.

4.3. O5 / Design

For the 3-detector HLV network, we find only a moderate $\lesssim 5\%$ difference in the number of detected events above our SNR threshold as the Virgo sensitivity is varied (left column Figure 3), though the localization distributions noticeably shift. We estimate that up to 20% (13%) of all detected BNS will have 90%-credible sky areas $\lesssim 10\text{deg}^2$ for the high (low) sensitivity Virgo projections. We expect up to 16% (8%) of signals detected 20s early and 13% (4%) of signals detected 40s early to be localized to $\lesssim 100\text{deg}^2$.

LIGO-Aundha has an even larger impact. Its addition to the HLV network suggests we expect up to 80% of detected BNS to be localized to $\lesssim 10\text{deg}^2$ by merger, dropping to $\lesssim 3\%$ and $\lesssim 1\%$, respectively, 20s and 40s before merger. The addition of KAGRA operating at 125 Mpc has a small impact on both the detection and localization when compared to the AHLV network operating at 100% duty cycle. For this best case network, we also explicitly compute the evolution of the 90%-credible sky areas as a function of time before merger in Figure 5, in addition to the two fiducial early warning times, 20s and 40s, in Figure 3.

4.4. Duty cycle impact on localizations and detections

Included in Figure 3 is a comparison of networks operating at 100% vs 70% duty cycle². The real benefit to networks with a large number of detectors is clear. While at 100% duty cycle there is little difference in localizations produced by 4 and 5-detector networks, there is a large benefit for networks that can only operate at moderate duty cycles. A 4-detector network at 70% duty cycle operates with all 4 detectors only 24% of the time; for a 5-detector network, there are at least 4 detectors active 53% of the time. The extra detector greatly increases the robustness of the global detector network. This effect is well demonstrated by the O5AHLV_{high} and O5AHKLV_{high} curves in the right panels of Figure 3.

² Chosen to match the duty cycle in the LVK’s observing scenario document (Abbott et al. 2021e).

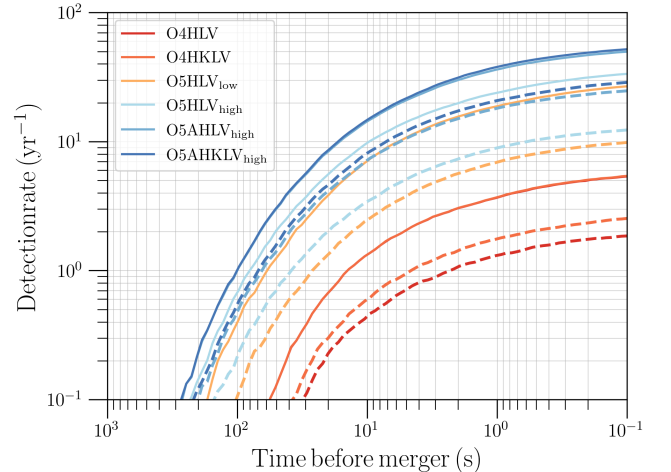


Figure 4. The expected number of detections per year vs the time detected before merger. Latencies associated with data acquisition, transfer, analysis, and enrichment are not included. The solid (dashed) lines show expectations for 6 different networks operating at 100% (70%) duty cycle. The solid lines of O4HKLVK and O5AHKLV_{high} lie directly on top of the respective networks without KAGRA, O4HLV and O5AHLV_{high}. All lines assume a median BNS merger rate of $470\text{Mpc}^{-3}\text{yr}^{-1}$. We do not include uncertainties associated with that measurement in this plot.

The impact on detection is also easily visualized. Figure 4 shows the expected number of detections at a fiducial BNS rate of $470\text{Gpc}^{-3}\text{yr}^{-1}$ for networks operating at 100% and 70% duty cycles, respectively. In all scenarios considered, down time decreases the number of expected detections by a factor of a few.

5. OUTLOOK AND DISCUSSION

Early warning detection will facilitate the capture of prompt, rapidly fading emission associated with BNS mergers. We find that even the most optimistic scenarios for O4 predict ~ 1 BNS detected before merger per year, with localizations $\gtrsim 100\text{deg}^2$. These detections will likely be too poorly localized for optical facilities to follow-up. We expect wide-field observatories such as the Murchinson Wide Field Array (Tingay et al. 2013) and the space-based Fermi Gamma-ray Burst Monitor (Meegan et al. 2009) and Neil Gehrels Swift Observatory (Gehrels et al. 2004) to benefit most from early warning detection with poor localizations. Indeed, new observational modes enabled with the Murchinson Wide Field Array will allow tests of BNSs as possible progenitors of non-repeating fast radio bursts (James et al. 2019), and will probe longstanding predictions tying fast radio bursts to pre-merger magnetosphere interactions (Hansen & Lyutikov 2001).

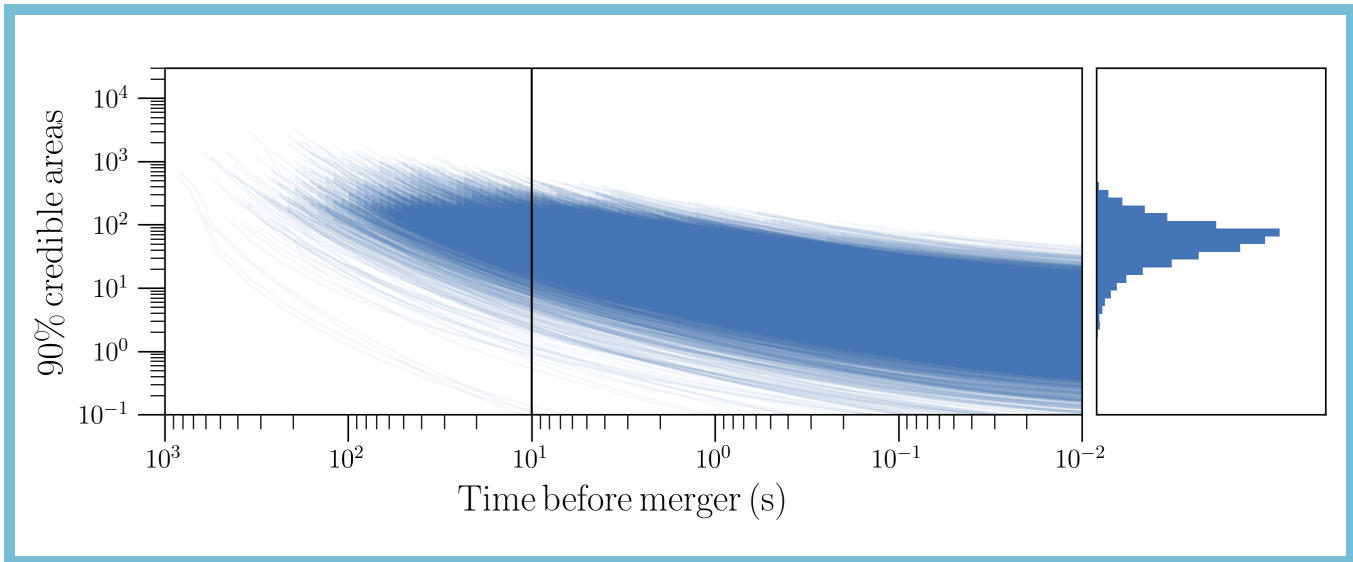


Figure 5. Here we show the expected 90% confidence areas as a function of detected time before merger for an idealized, design AHKLV network acting at 100% duty cycle. Each line tracks one simulation. The right part shows a histogram of expected localizations at the time indicated by the vertical black line (e.g. 10s before merger). At 10 s before merger, we expect most events to have localizations $\mathcal{O}(100 \text{ deg}^2)$. By merger, this improves to $\mathcal{O}(1 \text{ deg}^2)$. Simulations are only tracked once a network SNR ≥ 15 is reached. An animation of this figure that depicts the localization evolution is available [online](#).

Swift’s ability to rapidly localize will facilitate observations of near-merger X-ray emission, and recent Swift/BAT updates (Tohuvavohu et al. 2020) will enable subthreshold gamma-ray burst detections. Prompt X-ray observations could help reveal the immediate aftermath of the coalescing objects, and subthreshold detections could identify off-axis gamma-ray bursts and help probe the jet structure associated with these mergers. Similarly, observations by the Fermi Large Area Telescope would help complete our understanding of high-energy gamma-ray emission; in fact the telescope had powered down just before GRB170817A, which occluded measurements at energies $\gtrsim 100 \text{ MeV}$ (Kocevski et al. 2017).

By O5, early warning detections will become more common with up to ~ 10 detections made 10s before merger per year. Depending on network configuration and duty cycle, we expect that up to 80% of these will be localized to $\lesssim 10 \text{ deg}^2$, making them a prime target for optical facilities that cover $\mathcal{O}(1-10) \text{ deg}^2$, such as the Zwicky Transient Facility (Graham et al. 2019), Dark Energy Camera (Flaugher et al. 2015), and the highly anticipated Vera C. Rubin Observatory (Ivezić et al. 2019). Although previous optical observations were able to capture the kilonova associated with GW170817, it was already fading and clouded a complete understanding of the nature of the blue ejecta (Nicholl et al. 2017; Cowperthwaite et al. 2017). Chase et al. (2021) provides an in depth review of kilonova detectability prospects

across multiple observing bands for a selection of current and planned wide field-of-view observatories.

Other works have also estimated sensitivities and localization prospects for early warning detection of BNS for specific sensitivities and 100% duty cycles. We find that when our SNR detection threshold is modified to match those works, we obtain similar results in the 100% duty cycle limit. Sachdev et al. (2020) considered an HLV network operating at design sensitivity, finding that $\mathcal{O}(0.1 - 1)\%$ of all detected BNS events will be detected early with localizations $\lesssim 100 \text{ deg}^2$. If we impose a detection threshold of SNR 10, corresponding to the top 99% of recovered events in their study, we obtain similar expected localizations. Nitz et al. (2020a) also considered HLV, HKLV, and AHKLV networks from the “design” to “Voyager” eras of ground based detectors. We find that the distributions we present in Figure 3 for the O5HLV and O5AHLV networks are consistent with the distributions they find at SNR 10 in their Figure 3. This is complicated by the fact that we use slightly different sensitivity curves.

The observing scenarios document most recently produced by the LVK (Abbott et al. 2020b) does not consider early warning prospects, but we can compare our 0s early prospects to theirs. Their predictions for O4 considered the same HKLV network at 70% duty cycle with one major difference: KAGRA was assumed to reach 80 Mpc sensitivity. $\sim 40\%$ ($\sim 14\%$) of detected events were predicted to have 90%-credible sky areas smaller than 20 (5) deg^2 . We find that this matches

our predictions in the bottom right panel of Figure 3 which assumes a detection threshold of SNR 15 and a duty cycle of 70%. If we drop our SNR threshold to 12 to match the observing scenario document, we find slightly poorer constraints, likely attributable to the less sensitive KAGRA used in our network.

Although our results agree with similar studies, we caution that the specifics of the predicted distributions are highly dependent on the SNR threshold used for recovery. As shown in Section 4.1, we expect this method to consistently agree to within a factor of a few at the 50% level though Figure 2 shows that there is bias in the predicted distribution. Our detection threshold of 15 ensures that we 1) conservatively estimate the detection rate and 2) obtain reasonably accurate localization distributions. We have limited our study to the current generation of ground-based detectors, but others have considered early warning prospects for networks that include Cosmic Explorer and the Einstein Telescope (Akcaay 2019; Chan et al. 2018; Nitz & Dal Canton 2021). We leave further studies of these configurations to future work.

6. ACKNOWLEDGMENTS

LIGO was constructed by the California Institute of Technology and Massachusetts Institute of Technology with funding from the National Science Foundation and operates under cooperative agreement PHY-1764464. This paper carries LIGO Document Number LIGO-P2200010. The authors are grateful for computational resources provided by the LIGO Laboratory and supported by National Science Foundation Grants PHY-0757058 and PHY-0823459. SB further acknowledges support from the Deutsche Forschungsgemeinschaft (DFG), project MEMI number BE6301/2-1, and NSF grant PHY-1836779. We thank Surabhi Sachdev for providing a careful review of this manuscript, and BS Sathyaprakash for useful comments. RM gratefully acknowledges productive conversations with Shreya Anand and Derek Davis.

REFERENCES

- Aasi, J., et al. 2015, *Class. Quant. Grav.*, 32, 074001
- Abbott, B. P., et al. 2016, *Phys. Rev. Lett.*, 116, 061102
- . 2017a, *Phys. Rev. Lett.*, 119, 161101
- . 2017b, *Astrophys. J. Lett.*, 848, L12
- . 2019, *Phys. Rev. X*, 9, 031040
- . 2020a, *Astrophys. J. Lett.*, 892, L3
- Abbott, B. P., Abbott, R., Abbott, T., et al. 2020b, *Living reviews in relativity*, 23, 1
- Abbott, R., et al. 2021a, *Phys. Rev. X*, 11, 021053
- . 2021b, arXiv:2108.01045
- . 2021c, arXiv:2111.03606
- . 2021d, *Astrophys. J. Lett.*, 915, L5
- . 2021e, arXiv:2111.03634
- Acernese, F., et al. 2015, *Class. Quant. Grav.*, 32, 024001
- Akcaay, S. 2019, *Annalen Phys.*, 531, 1800365
- Akutsu, T., et al. 2019, *Nature Astron.*, 3, 35
- Ashton, G., et al. 2019, *Astrophys. J. Suppl.*, 241, 27
- Balasubramanian, R., Sathyaprakash, B., & Dhurandhar, S. 1996, *Phys. Rev. D*, 53, 3033, [Erratum: *Phys.Rev.D* 54, 1860 (1996)]
- Barack, L., & Cutler, C. 2004, *Phys. Rev. D*, 69, 082005
- Berry, C. P. L., et al. 2015, *Astrophys. J.*, 804, 114
- Blanchet, L., Damour, T., Esposito-Farese, G., & Iyer, B. R. 2005, *Phys. Rev.*, D71, 124004
- Blanchet, L., Damour, T., Iyer, B. R., Will, C. M., & Wiseman, A. 1995, *Phys. Rev. Lett.*, 74, 3515
- Borhanian, S. 2020, arXiv:2010.15202
- Buonanno, A., Iyer, B., Ochsner, E., Pan, Y., & Sathyaprakash, B. S. 2009, *Phys. Rev.*, D80, 084043
- Cannon, K., et al. 2012, *Astrophys. J.*, 748, 136
- Chan, M. L., Messenger, C., Heng, I. S., & Hendry, M. 2018, *Phys. Rev. D*, 97, 123014
- Chase, E. A., O'Connor, B., Fryer, C. L., et al. 2021, arXiv:2105.12268
- Cowperthwaite, P. S., et al. 2017, *Astrophys. J. Lett.*, 848, L17
- Cutler, C. 1998, *Phys. Rev. D*, 57, 7089
- Cutler, C., & Flanagan, E. E. 1994, *Phys. Rev. D*, 49, 2658
- Fairhurst, S. 2009, *New J. Phys.*, 11, 123006, [Erratum: *New J.Phys.* 13, 069602 (2011)]
- Finn, L. S. 1992, *Phys. Rev. D*, 46, 5236
- Finn, L. S., & Chernoff, D. F. 1993, *Phys. Rev. D*, 47, 2198
- Flaugher, B., Diehl, H. T., Honscheid, K., et al. 2015, *The Astronomical Journal*, 150, 150
- Gehrels, N., Chincarini, G., Giommi, P., et al. 2004, *The Astrophysical Journal*, 611, 1005
- Graham, M. J., et al. 2019, *Publ. Astron. Soc. Pac.*, 131, 078001
- Hansen, B. M. S., & Lyutikov, M. 2001, *Mon. Not. Roy. Astron. Soc.*, 322, 695
- Ivezić, v., et al. 2019, *Astrophys. J.*, 873, 111

- Iyer, B., et al. 2011, LIGO India, Tech. Rep. LIGO-M1100296, <https://dcc.ligo.org/LIGO-M1100296/public>
- James, C. W., Anderson, G. E., Wen, L., et al. 2019, Monthly Notices of the Royal Astronomical Society: Letters, 489, L75
- Kocevski, D., Omodei, N., & Vianello, G. 2017, arXiv:1710.05450
- Kovalam, M., Patwary, M. A. K., Sreekumar, A. K., et al. 2021, arXiv:2112.03597
- LVK. 2021, O4 Observing Plan Update: <https://www.ligo.org/scientists/GWEMalerts.php>, ,
- Magee, R., et al. 2019, *Astrophys. J. Lett.*, 878, L17
- . 2021, *Astrophys. J. Lett.*, 910, L21
- Meegan, C., Lichti, G., Bhat, P. N., et al. 2009, *ApJ*, 702, 791
- Nicholl, M., et al. 2017, *Astrophys. J. Lett.*, 848, L18
- Nitz, A. H., Capano, C., Nielsen, A. B., et al. 2019, *Astrophys. J.*, 872, 195
- Nitz, A. H., Capano, C. D., Kumar, S., et al. 2021, arXiv:2105.09151
- Nitz, A. H., & Dal Canton, T. 2021, *Astrophys. J. Lett.*, 917, L27
- Nitz, A. H., Schäfer, M., & Dal Canton, T. 2020a, *Astrophys. J. Lett.*, 902, L29
- Nitz, A. H., Dent, T., Davies, G. S., et al. 2020b, *Astrophys. J.*, 891, 123
- Olsen, S., Venumadhav, T., Mushkin, J., et al. 2022, arXiv:2201.02252
- Özel, F., & Freire, P. 2016, *Ann. Rev. Astron. Astrophys.*, 54, 401
- Pankow, C., Rizzo, M., Rao, K., Berry, C. P. L., & Kalogera, V. 2020, *Astrophys. J.*, 902, 71
- Poisson, E., & Will, C. M. 1995, *Phys. Rev. D*, 52, 848
- Rodriguez, C. L., Farr, B., Farr, W. M., & Mandel, I. 2013, *Phys. Rev. D*, 88, 084013
- Sachdev, S., et al. 2020, *Astrophys. J. Lett.*, 905, L25
- Saleem, M., et al. 2022, *Class. Quant. Grav.*, 39, 025004
- Sathyaprakash, B. S., & Dhurandhar, S. V. 1991, *Phys. Rev.*, D44, 3819
- Singer, L. P., & Price, L. R. 2016, *Phys. Rev. D*, 93, 024013
- Singer, L. P., et al. 2014, *Astrophys. J.*, 795, 105
- Singh, M. K., Kapadia, S. J., Shaikh, M. A., Chatterjee, D., & Ajith, P. 2021, *Mon. Not. Roy. Astron. Soc.*, 502, 1612
- Tingay, S. J., Goeke, R., Bowman, J. D., et al. 2013, *Publications of the Astronomical Society of Australia*, 30, e007
- Tohuvavohu, A., Kennea, J. A., DeLaunay, J., et al. 2020, *Astrophys. J.*, 900, 35
- Trovato, A. 2020, *PoS, Asterics2019*, 082
- Tsutsui, T., Nishizawa, A., & Morisaki, S. 2021, arXiv:2107.12531
- Vallisneri, M. 2008, *Phys. Rev. D*, 77, 042001
- Veitch, J., et al. 2015, *Phys. Rev. D*, 91, 042003
- Venumadhav, T., Zackay, B., Roulet, J., Dai, L., & Zaldarriaga, M. 2020, *Phys. Rev. D*, 101, 083030
- Washimi, T., Yokozawa, T., Tanaka, T., et al. 2021, *Class. Quant. Grav.*, 38, 125005
- Yu, H., Adhikari, R. X., Magee, R., Sachdev, S., & Chen, Y. 2021, arXiv:2104.09438
- Zackay, B., Venumadhav, T., Dai, L., Roulet, J., & Zaldarriaga, M. 2019, *Phys. Rev. D*, 100, 023007